AN ABSTRACT OF THE THESIS OF

Stephen Craig Moss II for the degree of Master of Science in Radiation Health Physics presented on August 3, 2000. Title: Calculation of Scanning Efficiencies for Portable Instruments Used to Detect Particulate Contamination.

Abstract approved: Redacted for Privacy

Kathryn A. Higley

Efforts are continually being made in remediation surveys to reduce the time and manpower required to perform work while maintaining the ability to detect low levels of contamination. To this end, organizations are utilizing portable instrumentation in conjunction with global positioning systems (GPS). This combination of technologies allows a surveyor to scan an area and record the count rate information along with the GPS coordinates. The data can then be mapped and cleanup efforts focused on areas that exceed set action levels. This study examined the effect of scanning speed on detector efficiency for four detectors and whether the scanning efficiency could be predicted. To accomplish this, a track was designed to allow a source to pass under the detector at speeds up to 1 m s^{-1}. To simulate the use of a GPS, a data-logger was used to collect the data for each run. Decreases in scanning efficiency were seen not only as the result of scanning speed but also as a function of signal processing. Results indicate that the scanning efficiency could be predicted using an equation that includes the static efficiency, detector diameter, the scanning speed, and the response time.

Calculation of Scanning Efficiencies for Portable Instruments Used to Detect Particulate Contamination

by

Stephen Craig Moss II

A Thesis Submitted
to
Oregon State University

In Partial Fulfillment of
The Requirements for the
Degree of

Master of Science

Presented August 3, 2000
Commencement June 2001

Master of Science thesis of Stephen Craig Moss II presented on August 3, 2000

APPROVED:

Redacted for Privacy

Major Professor, representing Radiation Health Physics

Redacted for Privacy

Head of the Department of Nuclear Engineering

Redacted for Privacy

Dean of the Graduate School

I understand that my thesis will become part of the permanent collection of Oregon State University libraries. My signature below authorizes releases of my thesis to any reader upon request.

Redacted for Privacy

Stephen Craig Moss II, Author

Acknowledgements

Dr. Kathryn Higley. As my advisor during my graduate work she has always been supportive and willing to help whenever I needed it.

Ludlum Instruments. The staff at Ludlum Instruments Inc. provided the rate meter/data-logger used in this study. This work could not have been performed without the use of their equipment and their technical support in understanding the operations of the equipment.

Oregon State University Radiation Safety Office. The Radiation Safety Office, directed by Rainier Farmer, provided the detectors and sources used in this study.

Department of Nuclear Engineering. The faculty and students of the Department of Nuclear Engineering were an invaluable source of ideas helping me formulate this work.

Contribution of Authors

Craig Marianno was involved in the design, and data collection for this project. This project was a continuation of the work he conducted for completing his Doctoral Degree.

Table of Contents

List of Figures

Calculation of Scanning Efficiencies for Portable Instruments Used to Detect Particulate Contamination

Craig Moss, Kathryn Higley, and Craig Marianno

Abstract

Efforts are continually being made in remediation surveys to reduce the time and manpower required to perform work while maintaining the ability to detect low levels of contamination. To this end, organizations are utilizing portable instrumentation in conjunction with global positioning systems (GPS). This combination of technologies allows a surveyor to scan an area and record the count rate information along with the GPS coordinates. The data can then be mapped and cleanup efforts focused on areas that exceed set action levels. This study examined the effect of scanning speed on detector efficiency for four detectors and whether the scanning efficiency could be predicted. To accomplish this, a track was designed to allow a source to pass under the detector at speeds up to 1 m s^{-1}. To simulate the use of a GPS, a data-logger was used to collect the data for each run. Decreases in scanning efficiency were seen not only as the result of scanning speed but also as a function of signal processing. Results indicate that the scanning efficiency could be predicted using an equation that includes the static efficiency, detector diameter, the scanning speed, and the response time.

Introduction

The technique of using portable instruments to survey areas for radiation contamination is standard practice. When trying to determine the presence of radioactive contamination, large areas can by surveyed quickly by “scanning” to establish the extent and location of contamination. Follow-up surveys are then used to quantify the amount of radioactive material actually present.

It has been demonstrated previously that an instrument’s detection efficiency can be, in part, a function of scanning speed, signal processing, and contaminant position in relation to the detector (Marianno, 2000). The purpose of the present study was to extend the work of Marianno to more practical applications, and answer the following questions. First, can an empirical relationship be developed that relates detector efficiency for portable detectors used to detect hot particles to the speed at which the detector is passed over the particle? Second, if so, is this relationship common for all detectors? Finally, what factors are important in developing this relationship?

The answers to these questions would be beneficial to individuals conducting large-area surveys for contamination. They would also be potentially useful when multiple types of detectors are used. Few studies have looked at the effects of scanning speed on instrument efficiency. (Sommers, 1975) looked at the ability of an operator to detect a source at slow scanning speeds, <15 cm s^{-1}. It was determined that an operator was more likely to detect a source when using the instrument's alarm settings while scanning at low speeds, <2.5 cm s^{-1}. At higher scanning speeds, 10-15 cm s^{-1}, the operator had a greater chance of detecting the source using the instrument's speaker output. For purposes of comparison, a fast-paced walk is 50 cm s^{-1}.

Using the instrument's speaker output requires interpretation of the audible signal by the operator. A recent study addressed the ability of a human operator to interpret the audible signal from a detector and determine whether contamination was present (Abelquest, 1999). An equation to calculate the minimal detectable concentration for an instrument using the detector's static efficiency and included a correction for the human operator was derived. However, neither Abelquest nor Sommers looked at the effect of scanning speed on detector efficiency.

Characterization surveys may be performed over large areas. To make these surveys less manpower and time intensive, portable instruments are being used in a scanning mode coupled with data logging and global positioning systems (GPS) (Berven, 1991; Egidi, 2000, Wrigth, 2000). The data collected from these surveys are downloaded into mapping software. Maps can be generated showing the location and extent of contamination for further characterization or cleanup.

Surveys using instruments coupled to data-loggers and GPS take count rate data directly from the instruments and store the output in the data-logger. These setups do not rely on interpretation of the count rate information by the human operator during the survey to determine the presence of contamination. The operator is only present to control the position of the detection equipment and the scanning speed. Therefore, scanning speeds must be chosen to ensure the instrument is capable of detecting potential contamination at the prescribed detection limit.

The physical parameters affecting the efficiency of portable detectors used in a scanning mode are essentially the same as when they are stationary. These parameters include energy of emission, background count rate, source strength, detector geometry, scanning speed, and response time of the meter. These parameters determine the probability that a particle or photon will interact in the detection volume and thus be counted. When the contamination source is large and uniformly distributed, the factors of speed and response time are negligible. However, these parameters must be considered when the scanning survey is attempting to detect discrete locations of contamination.

The present study was designed to determine the effect of scanning speed and changes in response time on the scanning efficiency of two sodium iodide (NaI) detectors, detecting the 60 keV photons of ^{241}Am, and two Geiger Mueller (GM) detectors, detecting the 662 keV photons of ^{137}Cs.

An additional intent of this study was to develop an empirical relationship to predict the scanning efficiency for these detectors under varying configurations.

Methods and Materials

Cart and Track System. A system was constructed that could repeatedly collect data at different scanning speeds while maintaining the same geometry. It was designed to be useful for different types of detection equipment. It was also constructed to have a low background radiation. A track system was designed so that a source could be moved under the test detector and shielding could then be placed around the detector to reduce background. Moving the source under the detector simulates a survey being conducted in the field during which the detector moves over the source.

A track 5.5 meters in length was built to move a 1 m by 1 m sled (Marianno, 2000) under the detector position (Fig. 1). The sled contained a 4-inch deep tray that contained approximately 1 inch of soil. The track was designed to provide adequate length to allow the sled to accelerate to a constant speed before traveling under the detector and then enough distance for the sled to come to a stop after moving out of the field of view of the detector. The sled was driven by a chain drive powered by a variable speed 1/6 horse power DC motor. Using this system the sled was able to reproducibly travel at speeds from 6 cm s^{-1} to over 100 cm s^{-1}.

Figure 1: Track system with Ludlum 2350-1 and a pancake GM detector. #1 is the track for the source sled, #2 is the Ludlum 2350-1 rate meter/data-logger, #3 is the pancake GM probe on the detector shelf, #4 is the light timer switch, #5 is the sled carrying the source.

A timing system consisting of a light switch and circuit board was designed to measure the time required for the sled to pass under the detector. The timer was placed on the track so that the speed of the sled would be determined at the detector's position on the track. The speed of the sled was then calculated using the length of the sled and the time of travel.

The source was placed on the surface of the soil in the sled so that the vertical distance from the active surface area of the detector was 4.5 cm. Additionally, a source position of 7.5 cm was also used with the end-window GM tube to compare changes in source height to detector response. The source distance was chosen to be large compared to the detector's diameter to reduce the effects of the solid angle.

Detectors. Four thin window detectors were selected as a representative sampling of instruments commonly used in field surveys. These detectors consisted of two NaI probes and two GM tubes. The NaI probes were the Alpha Spectra* FIDLER (SN: 03200A) and Ludlum† 44-3 (SN: PR053394). The GM probes were the Ludlum 44-7 (SN: PR078634) and Ludlum 44-9 (SN: PR022228).

The Alpha Spectra FIDLER is a NaI detector with a crystal that is 12.7 cm in diameter and 0.16 cm thick. A beryllium absorber 0.03 cm thick

* Alpha Spectra, 715 Arrowest Court, Grand Junction, Colorado, 81505.

† Ludlum Measurements, Inc., 501 Oak Street, P.O. Box 810, Sweetwater, Texas 79556, phone 800-622-0828

is in front of the crystal. The detector housing is 0.41 cm thick aluminum (Fig. 2a). Data were collected using a 4.8 μCi ^{241}Am source and a source to detector distance of 7.62 cm.

The Ludlum 44-3 is a NaI(Tl) Gamma Scintillator with 2.5 cm diameter by 0.1 cm thick crystal. The active and open window area is 5 cm^2 with a 3.8 cm magnetically shielded photomultiplier tube. The advertised sensitivity is ~675 cpm μR^{-1} hr for ^{125}I (Fig. 2b).[‡] Data were collected using a 4.8 μCi ^{241}Am source and a source to detector distance of 4.5 cm.

The Ludlum 44-7 is an end window halogen-quenched GM detector with an anodized aluminum housing (Fig. 2c). The active window area is 6 cm^2 with an open window area of 5 cm^2. The window thickness is 1.7±0.3 mg cm^{-2} mica. This detector has an advertised sensitivity of ~2100 cpm mR^{-1} hr for ^{137}Cs. Data were collected using a 4.4 uCi ^{137}Cs source and a source to detector distance of 4.5 and 7.5 cm.

The Ludlum 44-9 is a halogen-quenched pancake GM Detector with an aluminum housing and polyurethane enamel paint (Fig. 2d). The active window area is 15 cm^2 with an open window area of 12 cm^2. The window thickness is 1.7±0.3 mg cm^{-2} mica. This detector has an advertised sensitivity of ~3300 cpm mR^{-1} hr for ^{137}Cs. Data were collected using a 4.4 μCi ^{137}Cs source and a source to detector distance of 7 cm.

---

‡ Ludlum instrument specifications taken from the Ludlum webpage: www.ludlums.com

Rate Meter/Data-Logger. A Ludlum 2350-1 Data Logger (SN: 157660) with a data chip model #37122N27 was used as the rate meter. This meter was selected for its capability to be used with multiple detectors and its data-logging feature. The update interval of this instrument is the length of time between updates of the display and storage of a data point in the data-logger's memory. This time is 2 s. The count rate information in the data-logger's memory can be downloaded into spreadsheets or mapping software for subsequent analysis.

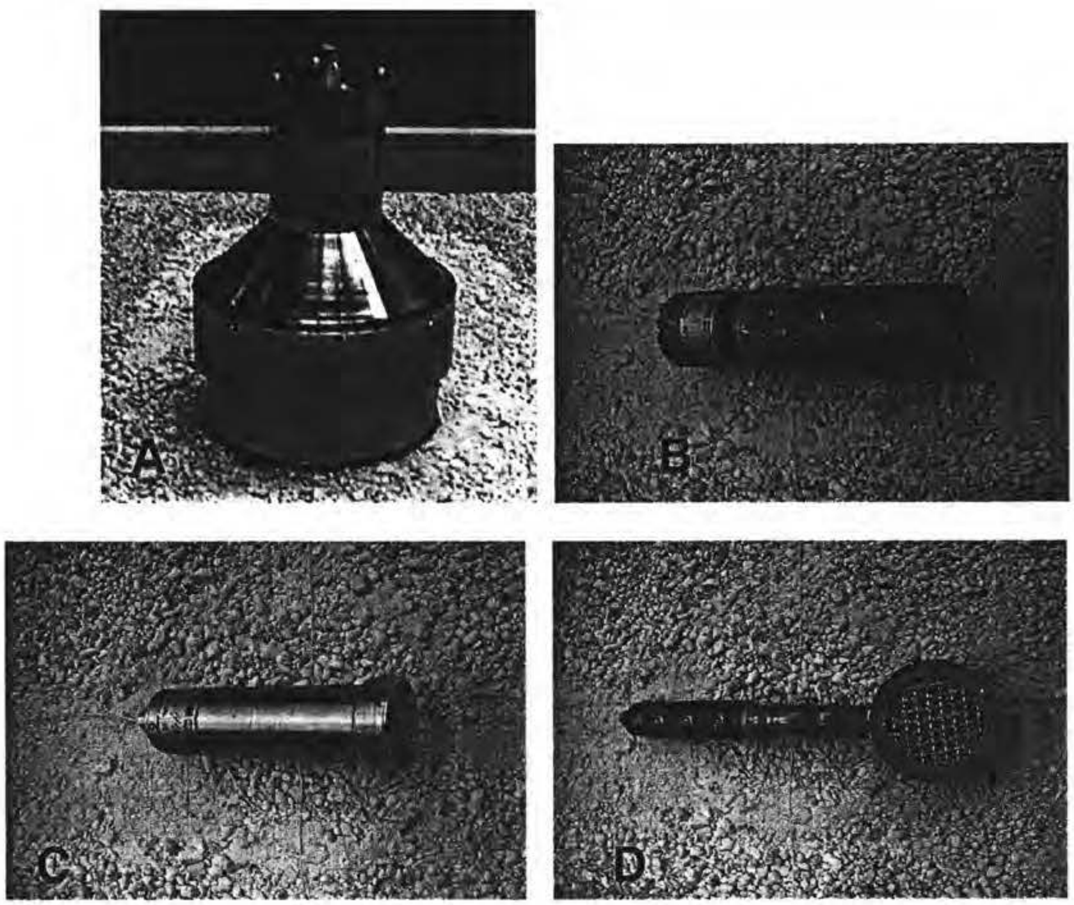

Figure 2a-d: Pictures of the four detectors used in this experiment. Figure A is the Alpha Spectra FIDLER, figure B is the thin-window NaI, figure C is the end-window GM, and figure D is the pancake GM.

One important aspect of the Ludlum 2350-1 is that its response time (R) can be changed to allow for a reduction in the statistical fluctuations of the data. The response time averages the count rate information over a preset period of time corresponding to:

$$\text{averaging time} = R * 2.718 \qquad \text{eq: 1}$$

For example, a response time of 1 s averages the data over the previous 2.718 s, while a 3 s response time averages the data over the previous 8.155 s. Because the response time was observed to effect the data collection, this study compared response time settings of 1, 3, and 5 s.

Data Acquisition/Analysis. As previously noted, data were collected by moving the source/sled under the stationary detector. The sled was positioned at the end of the track so the count rate at the detector was at background levels. The data-logger was turned on and allowed to collect data for one update interval, or 2 s, before the sled was moved. The sled was stopped after the source was 1.5 m past the detector. The data-logger was allowed to collect count rate information for 5 more counting intervals, or 10 s, before the acquisition was stopped to allow for the count rate to return to background levels. The scanning run was repeated 50 times for each detector and response time setting while varying the scanning speed.

The data collected were then downloaded into a spreadsheet. The scanning efficiency for each run was calculated as the ratio of the highest count rate recorded in any of the 2 s intervals divided by the expected source emissions:

$$E_s = \frac{\text{peak count rate during a scanning run (cpm) - bkg}}{\text{expected source emissions (dpm)}} \qquad \text{eq. 2}$$

where E_s is the scanning efficiency, and bkg is the background. Scanning runs were repeated at varying speeds and response time settings. The error in the count rate was calculated by:

$$Err_{cr} = \sqrt{\frac{\text{count rate}}{2 * \text{update interval}} + \frac{\text{bkg}}{2 * \text{update interval}}} \qquad \text{eq. 3}$$

where the update interval is 2 seconds (Cember, 1996). The standard error for each data point was then calculated by:

$$Err = E_s * \sqrt{\left(\frac{Err_{cr}}{\text{count rate}}\right)^2 + \left(\frac{\text{source emission error}}{\text{source emission}}\right)^2} \qquad \text{eq. 4}$$

Results and Discussion

It is expected that an instrument's ability to detect particulate contamination will decrease as the scanning speed increases. In essence, the instrument is spending less time in the vicinity of the source, and so will collect fewer counts. Another way to view the system is that a point source "looks" like a line source to the moving detector.

When scanning efficiency is plotted as a function of the scanning speed, one expects to see a decrease in the scanning efficiency as the speed is increased. This is borne out in repeated trials (Fig. 3a-d). These scanning efficiencies were measured using a 3 s response time. As the scanning speed approaches 1 m s^{-1} the count rate approaches background levels. This can be seen in Fig. 3a-d where the efficiency curve begins to flatten out and the counting error begins to increase. It should be noted that the decrease in scanning efficiency was similar for all four detectors. Since all the detectors responded in a similar fashion, the remainder of the discussion will focus on a single detector, the Ludlum 44-7 end-window GM.

Response time plays a significant role in scanning efficiency. As noted earlier, the data-logger requires the user to select a response time. The purpose of the response time is to dampen the "noise' in the detectors. However, it can impact the detector's scanning efficiency. Fig. 4a-c shows the difference in the scanning efficiency as the response time is increased, from 1 s to 5 s. It can be seen from Fig. 4a-c that as the response time is increased the scanning efficiency is decreased. It is also significant to note that there is a smoothing of the statistical fluctuations as the response time is increased.

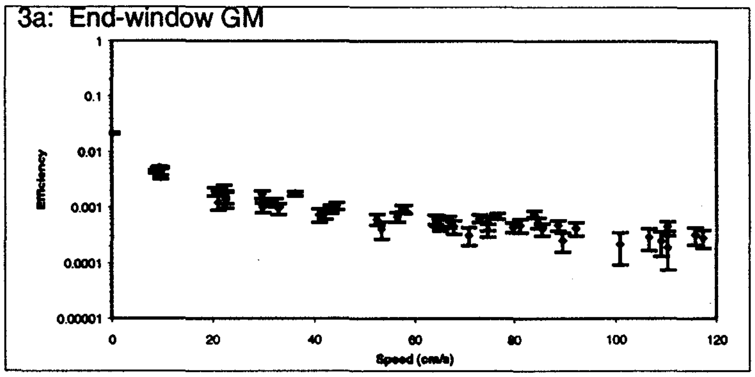

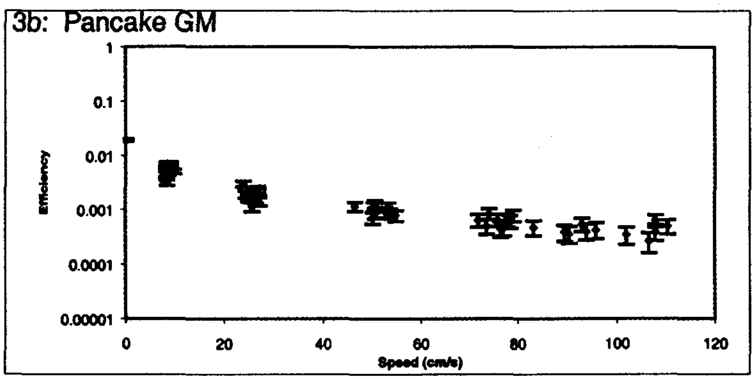

Continued

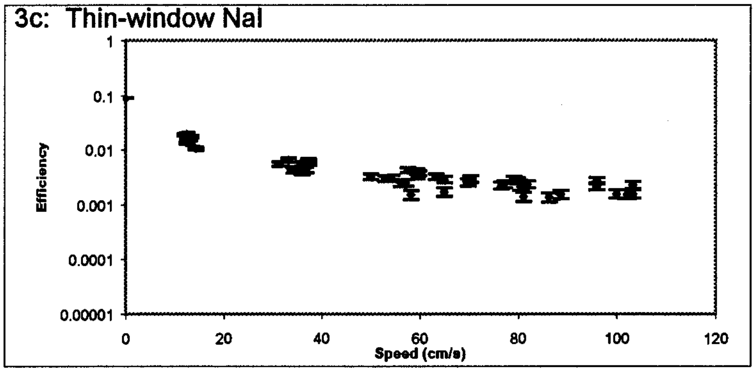

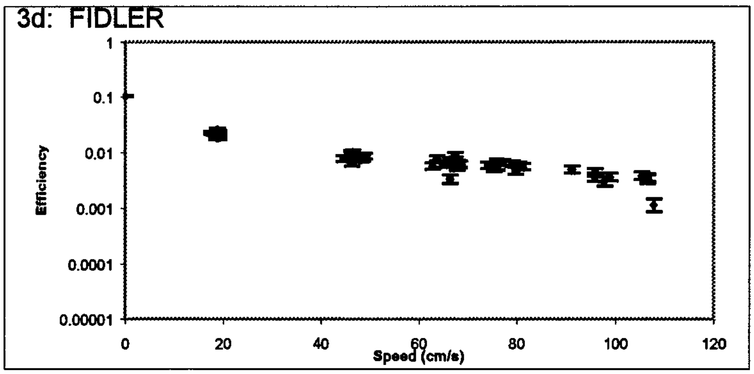

Figure 3a-d: Comparison of detection efficiency versus scanning speed. Response time settings of 3-seconds for the four detectors used; figure A is an End-window GM, figure B is a Pancake GM, figure C is a Thin-Window NaI, and figure D is a FIDLER. Each data point represents one scanning run with error bars showing 2 standard errors.

The response time algorithm in the Ludlum 2350-1 is set so the detector will react to increases and decreases in count rate roughly as a function of both the counting time and the response time setting. The function for this response algorithm is[§]:

$$P = 1 - e^{-(\frac{t}{R})} \quad \text{eq: 4}$$

[§] Mr. Richard Smoula, Ludlum Measurements Inc., 501 Oak Street, P.O. Box 810, Sweetwater, Texas 79556 where P is the fraction of peak static count rate observed in elapsed time, t and R is the response time. Thus as response time is increased, it takes longer for the count rate to reach its maximum value (Fig. 5). Fig. 5 shows that for a response time of 1 s, it takes 3 s for the count rate to reach 95% of its maximum value, 9 s for a response time of 3 s, and 15 s for a response time of 5 s.

To understand the effect of response time on scanning efficiency, the count rate data in a single scanning run at a speed of 30 cm s^{-1} was examined (Fig. 6). When the instrument is used in the scanning mode, the count time is limited to the update interval, or 2 s in this case, since the source is under the detector for less time than the update interval. It can be seen that as the response time is increased, lower count rates are recorded. In comparison, in the static mode with the detector positioned directly over the source, the observed maximum count rate was 30,300 cpm. With a nominal scanning speed of 30 cm s^{-1} (a slow walk) and the fastest response time (R = 1) there is a 4-fold decrease in efficiency.

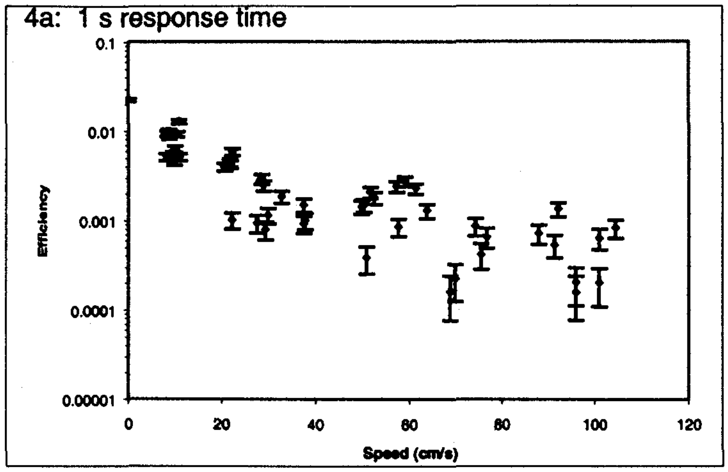
4a: 1 s response time
0.1
0.01
0.001
0.0001
0.00001
Efficiency
0
20
40
60
80
100
120
Speed (cm/s)

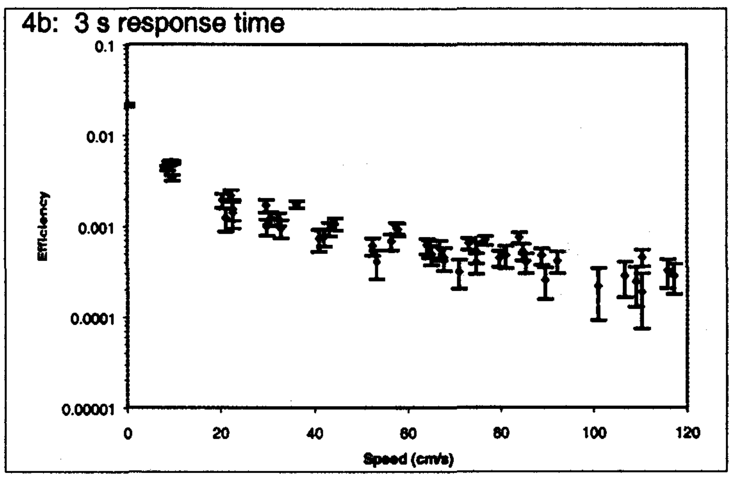
4b: 3 s response time
0.1
0.01
0.001
0.0001
0.00001
Efficiency
0
20
40
60
80
100
120
Speed (cm/s)

Continued

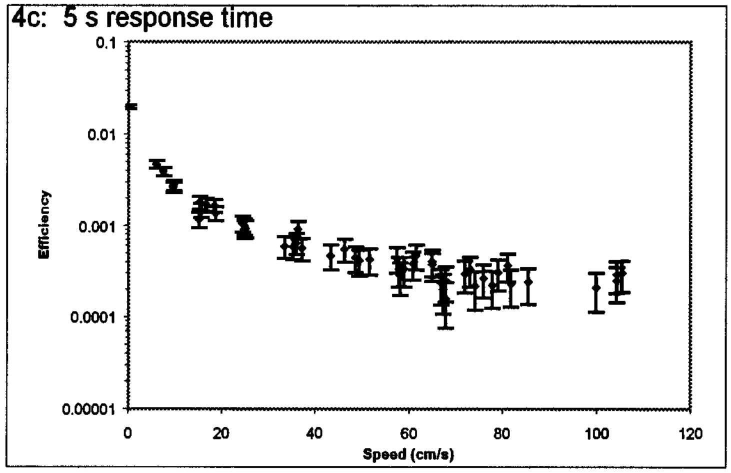

Figure 4a-c: Comparison of the effects of signal processing on detector efficiency as a function of scanning speed. Figure A is a response setting to 1-second, figure B is a response setting of 3-second, and figure C is a response setting of 5-second. Each data point represents one scanning run with error bars showing 2 standard errors.

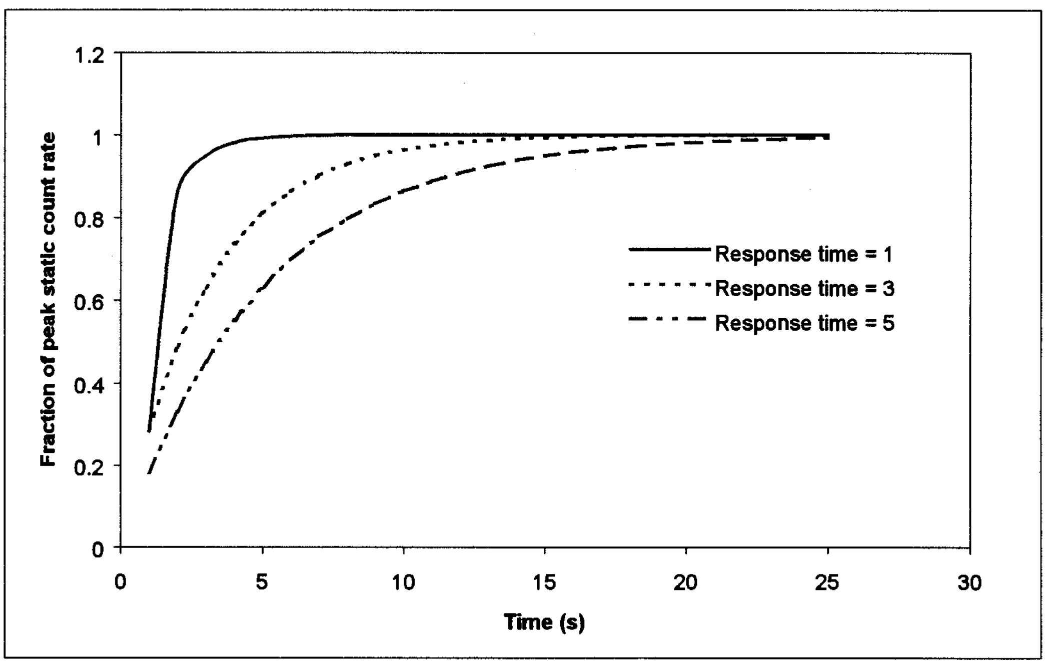

Figure 5: Theoretical static count rate as a function of elapsed time for three response time settings.

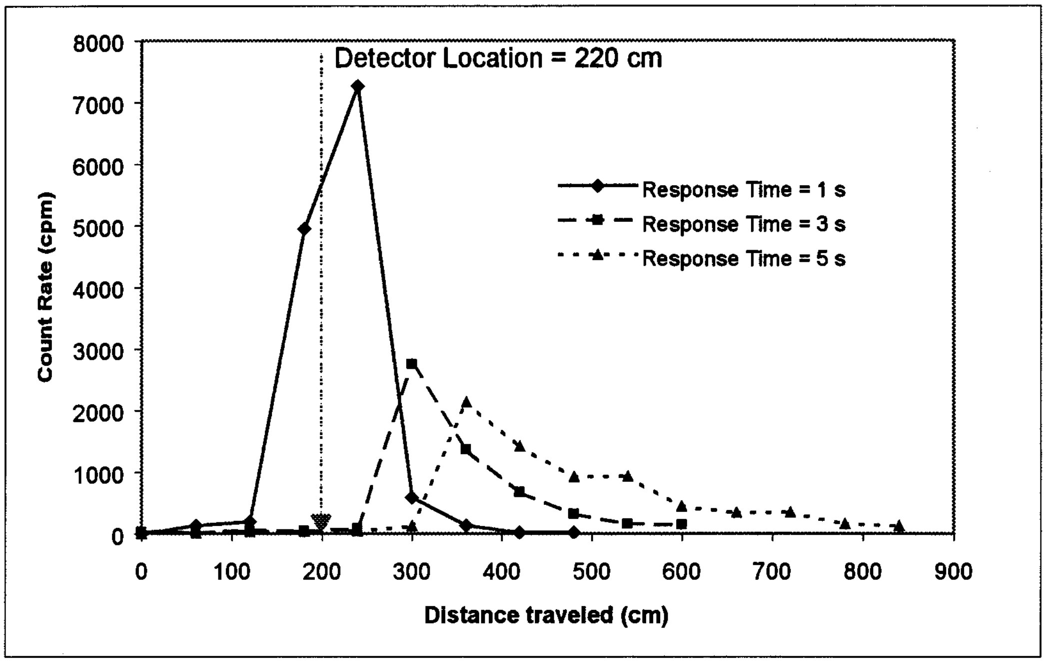

Figure 6: Comparison of count rate data for different response times at a nominal scanning speed of 30 cm s^{-1}. As the response time is increased, the count rate recorded in a single update interval decreases (Foldiak, 1986). The detector is positioned 220 cm from the start of the scan.

Additionally it is interesting to note the shift in the location of the peak count rate as the response time is increased. For this work the detector was located 220 cm from the starting point along the track. For the fastest response time the surveyor is approximately 20 cm past the source before the maximum count rate is reached and this situation gets worse with slower response times.

Another consideration in count rate fluctuations during a scanning interval is the position of the source during the update period. We can consider two extremes for this: first the source passes under the detector at the middle of the update period; this is considered the best case. Second, the source passes under the detector at the beginning (or end) of the update period; this is the worst case (Fig. 7). Optimally, one wants to maximize the count rate. However, during scanning surveys the position of the source during the scan is random. Choosing longer response times reduces the effect of source position. This can be seen in Fig. 2; as the response time increases, fluctuations in the count rate decreases.

The primary objective of this research was to determine if an empirical relationship could be developed that relates detector efficiency to scanning speed and response time. As noted earlier, all four detectors exhibited similar decreases in scanning efficiency as a function of scanning speed and response time setting. Therefore, developing an empirical relationship is feasible. The following section details the author's efforts to develop the equations.

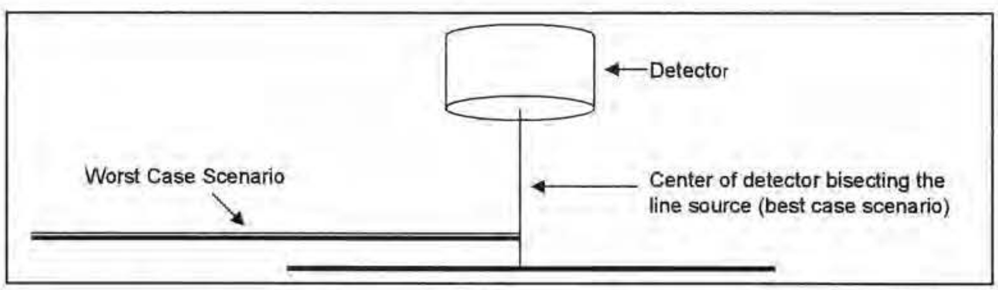

Figure 7: Best and worst case scenarios for position of particulate contamination. The highest count rate should be recorded when the detectors centerline is centered on the source's path length. The lowest count rate would be recorded when the end of the source path length passes under the centerline of the detector during the counting interval.

During a scanning interval, the source will pass in the vicinity of the detector at a given velocity. The time the source is directly beneath detector is related to velocity and the distance traveled by:

$$t = \frac{d}{v} \qquad \text{eq. 5}$$

where d is the distance traveled during the update internal and v is the velocity.

Substituting t from eq. 5 into eq. 4 one gets an expression for the response time in terms of distance traveled during the update interval and scanning speed:

$$P = 1 - e^{-(\frac{d}{v*R})} \qquad \text{eq. 6}$$

When the scanning speed is equal to zero, the scanning efficiency is equal to the detector's absolute static efficiency (E_a). By incorporating the absolute static efficiency into the equation the other parameters affecting detector efficiency (energy of emission, background count rate, source strength, and detector geometry) can be accounted for in the equation. When any of these parameters are changed, the static efficiency must change.

When the correction for signal processing and scanning speed are introduced, the static efficiency is reduced by the factor of P making eq. 6:

$$E_s = E_a * (1 - e^{-(\frac{d}{v*R})}) \qquad \text{eq. 7}$$

When d was set equal to the detector diameter and this equation was compared to the experimental data, it under-predicted the data when the source to detector distance was greater than or equal to the detector diameter. However, it accurately predicted the data when the source to detector distance was less than the detector diameter. Eq. 7 was therefore modified using a factor of the 2 times the detector diameter making it:

$$E_s = E_a * (1 - e^{-(\frac{2*d}{v*R})}) \qquad \text{eq. 8}$$

Equation 8 was found to fit the experimental data when the source to detector distance was greater than the detector diameter. The predicted results using eqs. 7 and 8 can be seen plotted with the experimental data in Fig. 8. As can be seen from Fig. 8 there is good agreement between the predicted and experimental data.

Conclusion

The equations developed in this study were designed to predict the scanning efficiency when using the signal processing used by Ludlum instruments, for the detection of discrete particulates, for thin window detectors. Other research is needed to evaluate volume detectors, the signal processing used with other meters, sources of varying sizes, and surface versus buried sources.

The ability to calculate an instrument's detection efficiency at various scanning speeds is essential. This study has demonstrated that it is possible to predict the scanning efficiency as a function of scanning speed and response time. The calculated scanning efficiency can be included in calculations to determine the instrument's minimal detectable concentration, and more complete planning of scanning surveys can be performed. The equations developed here work with the signal processing used by Ludlum Instruments. Equations will have to be developed to account for the signal processing of other instruments.

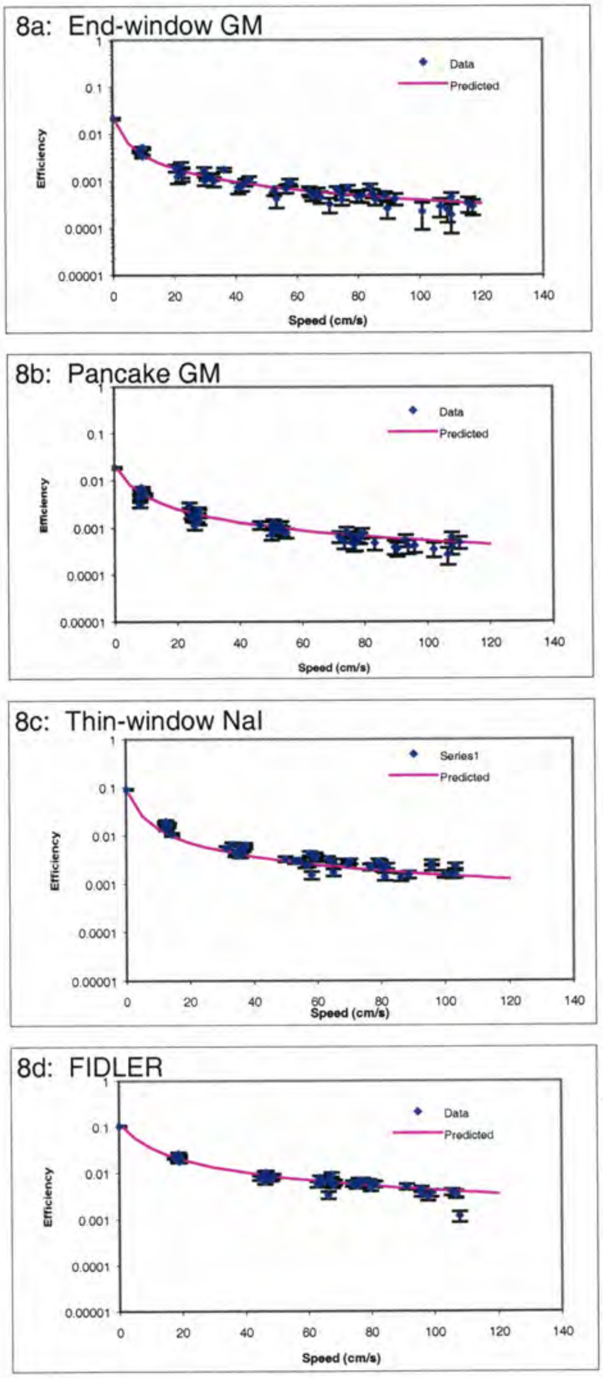

Figure 8a-d: Comparison of detector efficiency versus scanning speed for experimental data and predicted equations for the four detectors used; figure A is the End-Window GM, figure B is the Pancake GM, figure C is the Thin-Window NaI, and figure D is the FIDLER. Each data point represents one scanning run with error bars showing 2 standard errors.

References

Abelquist, E. W.; Brown, W.S.; Powers, G.E.; Huffert, A.M. Human performance in radiological survey scanning. Washington, DC: U.S. Nuclear Regulatory Commission; NUREG-6364; 1997

Abelquist, E. W.; Brown, W.S.; Powers, G.E.; Huffert, A.M. Minimum detectable concentration with typical radiation survey instrument for various contaminants and field conditions. Washington, DC: U.S. Nuclear Regulatory Commission; NUREG-1507; 1998.

Abelquist, E.W.; Brown, W.S. Estimating minimum detectable concentrations achievable while scanning building surfaces and land areas. Health Physics 76:3-10; 1999.

Berven, B.A.; Little, C.A.; Blair, M.S. A method to automate radiological surveys: the ultrasonic ranging and data system. Health Physics. 60:367-373; 1991.

Bevington, P.H.; Robinson, D.K. Data Reduction and Error Analysis for the Physical Sciences. McGraw-Hill, Inc, 1992.

Cember, H. Introduction to Health Physics, third edition. McGraw-Hill, Inc. 1996.

Chambles, D.A.; Dubose, S.S.; Sensitaffar, E.L. Detection limit concepts: foundations, myths, and utilization. Health Physics. 63:338-340; 1992.

Egidi, P.V.; Jensen, M.K.; Jones, A.R; Wilson-Nichols, M.J.; Smith, S.M.; Pierce, G.A.; Zutmanm, J.L. Use of global positioning systems for accelerated independent verification of cleanup at a superfund site. Proceeding of the 33rd Midyear Topical Meeting of the Health Physics Society. Medical Physics Publishing. Madison, Wisconsin. Feb 2000.

Foldiak, G., Industrial Application of Radioisotopes, Elsevier Science Publishers, 1986.

Knoll, G.F. Radiation Detection and Measurement, second edition, John Wiley and Sons, Inc., 1989.

Marianno, C.M.; Higley K.A. *An Experimental Determination of FIDLER Scanning Efficiency at Specific Speeds* in: An Examination of the Scanning Detection Efficiency of the FIDLER in Relation to Data Logging and Global Positioning Technology , PhD dissertation, Oregon State University, Corvallis, Oregon, June 2000

Press, W.H.; Flannery, B.P.; Teukolsky, S.A.; Vetterling, W.T. Numerical Recipes, the Art of Scientific Computing. Cambridge University Press, 1986.

Shleien, B. The Health Physics and Radiological Health Handbook, Scinta, Inc. 1992.

Sommers, J.F. Sensitivity of G-M and ion chamber beta-gamma survey instruments. Health Physics 28:755-761; 1975.

Wrigth, K.C., Webber, F.L., Hiaring, C.M. Site characterization using the global positioning radiometric scanner system. Proceeding of the 33rd Midyear Topical Meeting of the Health Physics Society. Medical Physics Publishing, Madison, Wisconsin. Feb. 2000.